

**Hard x-ray spectroscopy of the itinerant magnets  $R\text{Fe}_4\text{Sb}_{12}$  ( $R=\text{Na, K, Ca, Sr, Ba}$ )**Bassim Mounssief Jr.,<sup>1</sup> Marli R. Cantarino,<sup>2</sup> Eduardo M. Bittar,<sup>3</sup> Tarsis M. Germano,<sup>2</sup>  
Andreas Leithe-Jasper,<sup>4</sup> and Fernando A. Garcia<sup>2</sup><sup>1</sup>*IQUSP, Universidade de São Paulo, São Paulo, São Paulo 05508-090, Brazil*<sup>2</sup>*IFUSP, Universidade de São Paulo, São Paulo, São Paulo 05508-090, Brazil*<sup>3</sup>*Centro Brasileiro de Pesquisas Físicas, Rio de Janeiro, Rio de Janeiro 22290-180, Brazil*<sup>4</sup>*Max Planck Institute for Chemical Physics of Solids, D-01187 Dresden, Germany* (Received 19 September 2018; revised manuscript received 28 December 2018; published 28 January 2019)

Ordered states in itinerant magnets may be related to magnetic moments displaying some weak local moment characteristics, as in intermetallic compounds hosting transition metal coordination complexes. In this paper, we report on the Fe  $K$ -edge x-ray absorption spectroscopy (XAS) of the itinerant magnets  $R\text{Fe}_4\text{Sb}_{12}$  ( $R = \text{Na, K, Ca, Sr, Ba}$ ), aiming at exploring the electronic and structural properties of the octahedral building block formed by Fe and the Sb ligands. We find evidence for strong hybridization between the Fe  $3d$  and Sb  $5p$  states at the Fermi level, giving experimental support to previous electronic structure calculations of the  $R\text{Fe}_4\text{Sb}_{12}$  skutterudites. The electronic states derived from Fe  $3d$ –Sb  $5p$  mixing are shown to be more occupied and/or less localized in the cases of the magnetically ordered systems, for which  $R = \text{Na}$  or  $\text{K}$ , connecting the local Fe electronic structure to the itinerant magnetic properties. Moreover, the analysis of the extended region of the XAS spectra (EXAFS) suggests that bond disorder may be a more relevant parameter to explain the suppression of the ferromagnetically ordered state in  $\text{CaFe}_4\text{Sb}_{12}$  than the decrease of the density of states.

DOI: [10.1103/PhysRevB.99.035152](https://doi.org/10.1103/PhysRevB.99.035152)**I. INTRODUCTION**

Magnetically ordered states in itinerant magnets are understood to be connected to a magnetic instability due to a high density of states at the Fermi surface, thus being a property of itinerant electronic states. This is in contrast to the magnetic properties of insulators which stem from localized electronic states [1,2].

Although this formal division of magnetism from either itinerant or localized moments offers an important rationalization of the problem, it is striking that there are only a few solids hosting magnetically ordered states for which the magnetic properties bear no relation whatsoever to atomic electronic properties. To our knowledge, examples include  $\text{ZnZr}_2$  [3],  $\text{ScIn}_3$  [4], and the recently discovered  $\text{AuTi}$  [5]. In general, magnetic moments in itinerant magnets may display weak local moment characteristics [2].

The iron-based superconductors [6] illustrate an example of itinerant magnets for which the specific Fe orbital configuration, valence, and coordination structure are important parameters. In this broad research field, the presence of a structural building block, featuring Fe atoms in tetrahedral coordination, is a common thread. The experimental investigation with x-ray absorption spectroscopy (XAS) of the electronic and structural properties of this coordination structure brought to light several questions in the field, including the role of transition metal substitution [7–9], bond disorder [10–13], and the relevance of Mott physics [14].

As opposed to the case of local moment magnets [1], it is not clear at which situation the electronic and structural properties of a coordination structure will be relevant to the magnetic properties of itinerant magnets. In fact, it is

expected that in many situations the conduction electrons will completely screen the effect of the ligands [2]. The experimental investigation of itinerant magnets hosting coordination structures may challenge this understanding, opening a new perspective to the study of itinerant magnets.

In this paper, we present Fe  $K$ -edge x-ray absorption spectroscopy (XAS) of the  $R\text{Fe}_4\text{Sb}_{12}$  ( $R = \text{Na, K, Ca, Sr, Ba}$ ) filled skutterudites. In the filled skutterudite structure [15], the metal ( $M$ ) is coordinated by 6 ( $X$ ) ligands (mainly  $X = \text{P, As, Sb}$ , although  $X = \text{Ge}$  is also possible), arranged in an octahedral geometry (see Fig. 1). Our Fe  $K$ -edge XAS experiments allowed a detailed study of the structural and electronic properties of the  $\text{FeSb}_6$  building blocks along the  $R = \text{Na, K, Ca, Sr, Ba}$  series.

This series of  $R\text{Fe}_4\text{Sb}_{12}$  filled skutterudites presents an interesting case study of skutterudite compounds for which electronic and magnetic properties are dominated by the transition metal magnetism [16–21]. A high density of states at the Fermi level ( $E_F$ ) is inferred based on the measured electronic contribution to the heat capacity  $\gamma$ , presenting values on the order of  $\approx 100 \text{ mJ mol}^{-1} \text{ K}^{-2}$ . Electronic structure calculations attribute the presence of such heavy quasiparticles at  $E_F$  to strongly hybridized Fe–Sb states at  $E_F$ . The alkaline metal filled skutterudites ( $R = \text{Na, K}$ ) present a ferromagnetic phase transition at the critical temperature ( $T_C$ ) about  $\approx 80 \text{ K}$ , whereas the alkaline earth filled ( $R = \text{Ca, Sr, Ba}$ ) ones remain paramagnetic for temperatures down to  $T = 2 \text{ K}$  [22–24].

A qualitative understanding of the evolution of the magnetic properties may be formulated in terms of the electron filling along the series. In reference to the fully compensated semiconductor  $(\text{CoSb}_3)_4$ , the  $(\text{FeSb}_3)_4$  framework is short of

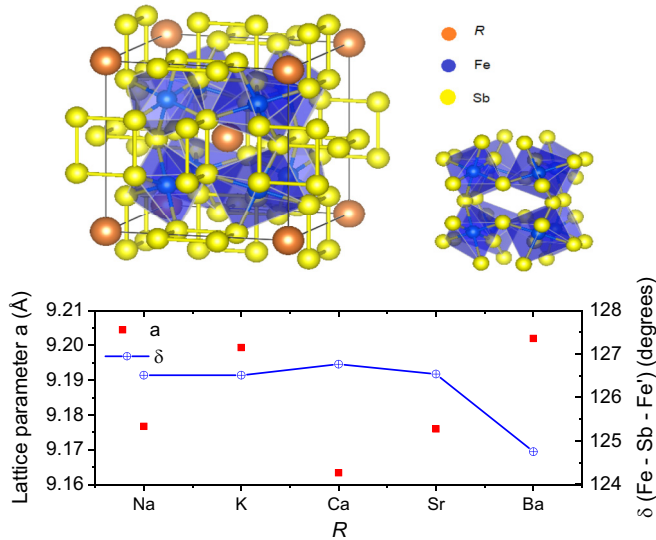


FIG. 1. Left: Ternary filled skutterudite structure (space group  $Im\bar{3}$ ) displaying the rectangular Sb-Sb rings and the  $FeSb_3$  distorted octahedra [28]. Right: Detail of the Fe-Sb octahedral coordination. Below: The lattice parameters  $a$  (red squares) and the Fe-Sb-Fe' bond angles  $\delta$  (blue line) along the series. It is noteworthy that in spite of the large variation of the cationic sizes,  $a$  changes only slightly along the series, evidencing that the  $Fe_4Sb_{12}$  framework is particularly stiff.

4 electrons. The stabilization of the structure is provided by electron transfer from the filler cation  $R$  [15,25]. However, the monovalent alkaline metal or divalent alkaline earth fillers can only partially compensate the host structure. Charge carriers in  $RFe_4Sb_{12}$  are, therefore, holes and, due to the extra electron, the alkaline earth filled systems present a smaller density of states at the Fermi level ( $E_F$ ). In turn, the Stoner factor should be less for the systems for which  $R = Ca, Sr, or Ba$ , suppressing the magnetic instability that gives rise to ferromagnetic order in the  $R = Na$  or  $K$  systems [24].

Electronic structure calculations do support this qualitative scenario, favoring an itinerant description of the magnetic properties of these skutterudites [24]. On the other hand, neutron scattering experiments of  $NaFe_4Sb_{12}$  could demonstrate the presence of local moments at the Fe sites [26] and further investigation of the electronic structure of  $NaFe_4X_{12}$  ( $X = P, As, Sb$ ) [27] revealed that the specific nature of the ligand orbitals ( $3p$  for  $P$ ,  $4p$  for  $As$ , or  $5p$  for  $Sb$ ) implies a relevant effect in the size of the magnetic moment and the nature of the magnetic instability. These two results suggest that local properties of the  $FeSb_6$  coordination structure could relate to the evolution of the itinerant magnetism of the system.

## II. METHODS

High-quality polycrystalline samples of  $RFe_4Sb_{12}$  ( $R = Na, K, Ca, Sr, Ba$ ) skutterudites were synthesized by the solid state method [22]. Hard x-ray absorption spectroscopy experiments were performed at the XAFS2 [29] beamline of the Brazilian Synchrotron Light Source (CNPEM-LNLS). At the XANES region, the spectra were measured in steps of 0.3 eV in both fluorescence and transmission mode for the

light filler elements ( $R = Na, K, Ca$ ) whereas for the heavy fillers ( $R = Sr$  or  $Ba$ ) only the fluorescence mode was considered. The fluorescence signal was recorded by 11 Ge detectors and averaged to improve the signal-to-noise ratio. An Fe foil, kept at room temperature, was measured in the transmission mode as a reference throughout the experiments. A conventional He-flow cryostat was employed to achieve temperatures down to  $T = 10$  K. Each spectrum was measured 3 times.

Our interpretation of the results of the near-edge region of the XAS spectra (XANES) is supported by *ab initio* calculations of multiple scattering theory implemented by the FEFF8.4 code [30]. The *ab initio* calculations were performed adopting clusters of 226 atoms and the Hedin-Lundqvist pseudopotential to account for the exchange interaction. Self-consistent calculations were performed for a cluster radius of 6 Å. The calculations of the spectrum include only contributions of dipolar nature. The inclusion of quadrupolar contributions rendered a minute contribution to the pre-edge region, which was disregarded. Cluster size effects were investigated adopting  $NaFe_4Sb_{12}$  as a reference and no changes were observed for larger cluster sizes (up to 400 atoms). The effects of adopting larger clusters for the self-consistency calculations (up to 7 Å) were also tested but did not result in more accurate results. For the extended region of the XAS spectra (EXAFS), FEFF calculations were implemented along with IFEFFIT using the Demeter platform [31].

## III. RESULTS AND DISCUSSION

In Figs. 2(a) and 2(b) the Fe  $K$ -edge spectrum of  $NaFe_4Sb_{12}$  (XANES region), the respective FEFF simulation, and the spectrum of the Fe foil reference are presented [Fig. 2(a)] along with their energy derivatives [Fig. 2(b)]. Capital letters  $A$  and  $B$  mark the position of the main features of the  $NaFe_4Sb_{12}$  spectrum, respectively the pre-edge and edge transitions, determined by the inflection points of the spectrum. To match the experimental transition edge position (feature  $B$ ), the FEFF calculation was shifted by  $-4.3$  eV. Features  $A$  and  $B$  are only qualitatively reproduced by the FEFF calculation. In Fig. 2(a) it is shown that the simulation overestimates the edge jump (see discussion below) and in Fig. 2(b) it is suggested that the pre-edge transition splits into two components which, however, are not observed for  $NaFe_4Sb_{12}$ .

In the inset of Fig. 2(b), the energy region of the pre-edge is presented in detail and the energy derivatives of the spectra for  $NaFe_4Sb_{12}$  and  $CaFe_4Sb_{12}$  are compared with the respective FEFF simulations. For  $NaFe_4Sb_{12}$ , the spectrum presents only one maximum and flattens, while for  $CaFe_4Sb_{12}$  it presents a weak, however clear, second maximum (as indicated by the black arrows). The FEFF calculated splitting of the pre-edge amounts to  $\Delta E^{FEFF} \approx 1.2$  eV closely corresponding to the observed value of  $\Delta E^{R=Ca} \approx 1.3$  (0.3) eV, suggesting that the observed weak second maximum is an intrinsic property of the system. The  $NaFe_4Sb_{12}$  XANES spectrum compares well with the  $R = K$  spectrum while the pre-edge splitting observed at the  $CaFe_4Sb_{12}$  spectrum is also present for the  $R = Sr$  or  $Ba$  cases [see Fig. 4(a)], although the effect is weaker.

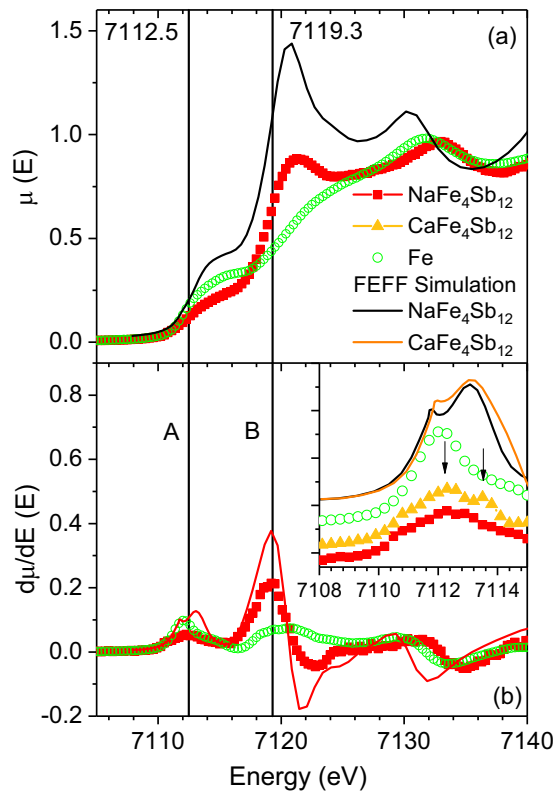


FIG. 2. (a) Fe  $K$ -edge XANES spectra for  $\text{NaFe}_4\text{Sb}_{12}$ , the reference Fe foil, along with FEFF calculations for  $\text{NaFe}_4\text{Sb}_{12}$ , and (b) the derivative of the same spectra. Two prominent features  $A$  and  $B$  are marked in reference to the maximum of the energy derivatives of the spectrum. In the inset, the  $\text{NaFe}_4\text{Sb}_{12}$  and  $\text{CaFe}_4\text{Sb}_{12}$  spectra (offset for better visualization) are compared. It is shown that a second maximum (black arrows) of the energy derivative can be observed for  $\text{CaFe}_4\text{Sb}_{12}$  but not for  $\text{NaFe}_4\text{Sb}_{12}$ . The overall shape of the spectrum is reminiscent of the Fe  $K$ -edge spectra obtained for  $\text{Fe}^{2+}$  oxides in octahedral coordination complexes.

Our FEFF simulations include only dipolar terms and thus we ascribe the pre-edge to a dipolar transition. There are two mechanisms that can account for a pre-edge intensity dominated by a dipolar transition, and these are (i) an Fe  $3d$ - $4p$  mixing (allowing an on-site dipolar Fe  $1s \rightarrow 3d$  transition) and (ii) a strong ligand  $np$  (in this case Sb  $5p$ ) mixing with the Fe  $3d$  orbitals (allowing an intersite Fe – Fe'  $1s \rightarrow 3d$  transition) [32–34]. If the Fe site is centrosymmetric, as in octahedral symmetry, the Fe  $3d$ - $4p$  mixing is exactly suppressed. Therefore, the pre-edge intensity should be taken as a piece of evidence for strong Fe  $3d$ -Sb  $5p$  mixing.

Since the Fermi level ( $E_F$ ) sits at the  $A$  feature, experimentally determined to be about  $E_F \approx 7112.5$  eV (for  $\text{NaFe}_4\text{Sb}_{12}$ ), our result offers compelling experimental evidence for a significant contribution of Sb  $5p$  orbitals at  $E_F$ . This contribution is key for understanding the presence of heavy quasiparticles at  $E_F$  in the  $R\text{Fe}_4\text{Sb}_{12}$  skutterudites, which are directly connected to their magnetic properties.

We caution, however, that in skutterudites the metal coordination is not that of a regular octahedron and, in addition, may contain a particularly large degree of disorder due to the unconventional vibrational dynamics of these systems [35–37].

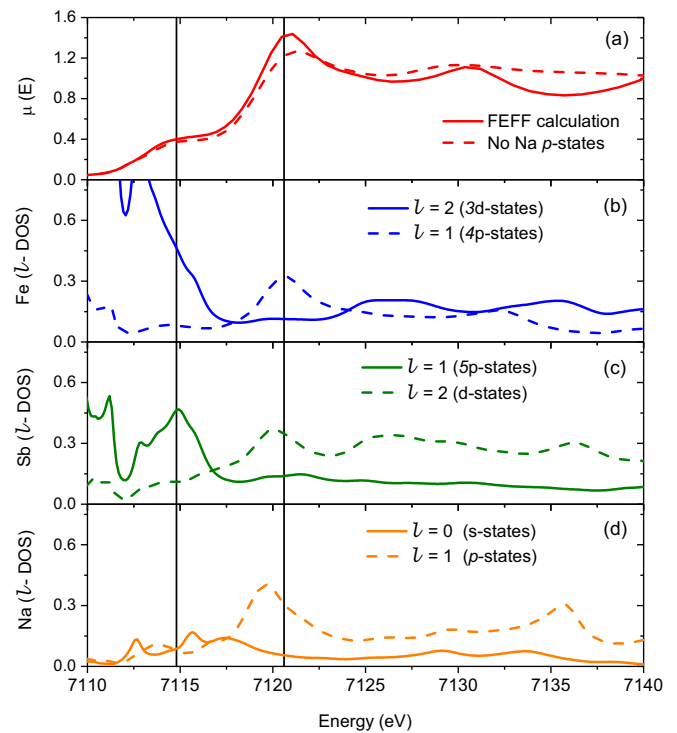


FIG. 3. (a) FEFF calculations of the XANES spectrum and (b)–(d) site projected  $l$ -DOS of Na, Fe, and Sb for  $\text{NaFe}_4\text{Sb}_{12}$ . The most relevant contributions are displayed. The main features of the XANES spectrum correlate well with the Fe  $4p$  (general), Sb  $5p$  ( $A$  feature), Sb  $d$  ( $B$  feature), and Na  $p$  ( $B$  feature) site projected density of states. The thick line is a guide to the eyes highlighting the contribution from Sb  $5p$  and Fe  $4p$  states.

Therefore, a contribution from Fe  $3d$ - $4p$  mixing to the pre-edge cannot be entirely discarded.

The  $B$  feature is absent in the Fe foil spectrum and reflects the Fe coordination structure. Indeed, the measured spectrum is reminiscent of the Fe  $K$ -edge spectra in systems containing  $\text{Fe}^{2+}$  cations in octahedral symmetry [34,38] and suggests that the Fe atoms in the investigated skutterudites are close to a  $2+$  formal valence state. This result supports the qualitative discussion on the electronic properties and bond scheme of the  $R\text{Fe}_4\text{Sb}_{12}$  [15,25] skutterudites. A more detailed understanding of the distinct contributions to the spectrum is attained by comparing the FEFF calculated spectrum with the site projected local density of states ( $l$ -DOS) for Fe, Sb, and Na. The results are presented in Figs. 3(a)–3(d).

The spectrum in Fig. 3(a) correlates well with the Fe  $4p$  contribution to the  $l$ -DOS. Thus, the Fe  $K$  edge can indeed be well described as a Fe  $1s \rightarrow 4p$  transition and, furthermore, it indicates that the distortion of the octahedral coordination allows a certain degree of Fe  $3d$ - $4p$  mixing that contribute to the pre-edge region. In addition, it is noteworthy that the pre-edge contains a large contribution from the Sb  $5p$  orbitals and that the  $B$  feature contains large contributions from Sb  $d$  and Na  $p$  states (or, in general,  $R p$  states).

Turning our attention to the  $B$  feature, we performed distinct FEFF calculations removing the Sb  $d$  orbitals and the Na  $p$  orbitals. Removal of the former leads to an overall decrease of the intensity of the spectrum. The removal of the

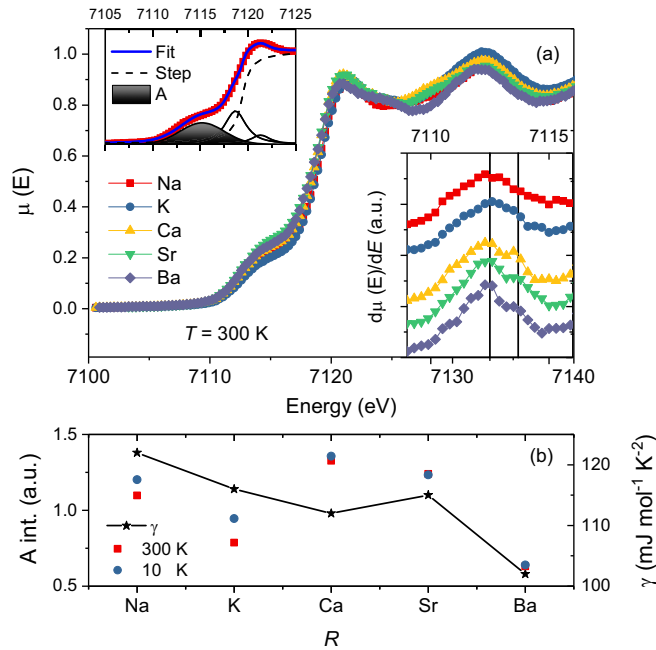


FIG. 4. (a) Fe  $K$ -edge XANES spectra for all  $R\text{Fe}_4\text{Sb}_{12}$  ( $R = \text{Na}, \text{K}, \text{Ca}, \text{Sr}, \text{Ba}$ ) skutterudites. Upper inset: Fitting of a representative spectrum, wherein we highlight a Gaussian curve describing the pre-edge. Lower inset: Detail of the energy derivative of the pre-edge transition for all samples. A second maximum can be observed for the  $R = \text{Ca}$  and likely for the  $R = \text{Sr}$  and  $\text{Ba}$  skutterudites. (b) Pre-edge transition intensity (peak area  $A$ , left axis) at  $T = 300 \text{ K}$  (red squares) and  $T = 10 \text{ K}$  (blue squares) and the  $\gamma$  coefficient (black line) of the electronic contribution to heat capacity (right axis, from Ref. [24]), both as a function of  $R$ .

$\text{Na}$   $p$  contribution (as can be observed) implies a much less intense  $B$  feature, without any other sizable effects. Similar calculations were run for all other fillers and these results are representative of what is observed for the whole series. This study allows the conclusion that the FEFF calculation overestimates the filler  $p$  contribution to the  $B$  feature. In all cases, a significant contribution of  $\text{Sb}$   $5p$  states to the pre-edge was found, giving extra support for the origin of the pre-edge intensity of the spectrum as above discussed. Having established the distinct contributions to the spectrum, we now turn to a comparison between the experimental results across the series.

The XAS experimental data in the XANES region of the  $R\text{Fe}_4\text{Sb}_{12}$  series are presented in Fig. 4(a). The lower inset shows in detail the pre-edge region for all samples. The splitting of the pre-edge observed for  $R = \text{Ca}$  is also apparent for the  $R = \text{Sr}$  or  $\text{Ba}$ , but is weaker. Again, we resort to the comparison with the respective FEFF calculations, which will also display a splitting of about  $\Delta E = 1.2 \text{ eV}$ , to trust that this weak effect is an intrinsic property of the system. Thus, the splitting of the pre-edge transition is indicated to be a characteristic of the nonmagnetically ordered compounds. If we now focus our attention back to Figs. 3(a)–3(d), a close inspection of the  $\text{Sb}$   $5p$  LDOS suggests that this contribution is the source of the pre-edge splitting. It is predicted for all  $R\text{Fe}_4\text{Sb}_{12}$ , but is observed only for the alkaline earth

filled systems. The result can be interpreted in terms of the distinct electronic occupation at  $E_F$  expected for the  $R\text{Fe}_4\text{Sb}_{12}$  skutterudites, since the presence of available states in the cases for which  $R = \text{Ca}, \text{Sr},$  or  $\text{Ba}$  allows the transition to the  $\text{Fe}$   $3d$ – $\text{Sb}$   $5p$  mixed orbitals close to  $E_F$ . Alternatively, it may relate to distinct  $\text{Fe}$   $3d$ – $\text{Sb}$   $5p$  mixing when the cases  $R = \text{Na}$  or  $\text{K}$  and  $R = \text{Ca}, \text{Sr},$  or  $\text{Ba}$  are compared. Therefore, the electronic states derived from  $\text{Fe}$   $3d$ – $\text{Sb}$   $5p$  mixing are either more occupied or less localized for the ferromagnetically ordered compounds.

No shift is observed in the pre-edge position (first inflection), as it is the case as well of the edge position. The lack of a shift in the pre-edge does not imply that  $E_F$  is constant across the series but rather that the extra electron resulting from alkaline earth filling will not sit at the  $\text{Fe}$  site. Indeed, a more involved scenario is in order, since it is expected that the extra electrons contributed by the alkaline earth will further stabilize the  $\text{Sb}$ – $\text{Sb}$  bonds. In general, one should be careful when tracking the destiny of the extra carriers due to electron or hole doping in itinerant systems. A similar situation was recently clarified in the case of the iron arsenides [9].

In Fig. 4(b) we present the pre-edge peak intensities (associated with the  $A$  feature) compared with the  $\gamma$  coefficient from heat capacity (from Ref. [24]). The upper inset of Fig. 4(a) display a representative result for the peak fitting procedure, wherein it is shown that only one Gaussian was adopted to fit the pre-edge transition.

In view of our interpretation of the pre-edge intensity, the data are capturing the evolution of the  $\text{Fe}$   $3d$ – $\text{Sb}$   $5p$  orbital mixing and occupation as a function of  $R$ , both of which are connected to  $\gamma$ . It is observed in Fig. 4(b) that, with the exception of the case of  $\text{CaFe}_4\text{Sb}_{12}$  (see discussion related to the EXAFS results), the intensities follow qualitatively the trend of the  $\gamma$  coefficient across the series, adding yet another piece of evidence in support of our interpretation of the pre-edge peak intensity.

Orbital mixing is strongly influenced, as well, by local structural parameters, such as  $\text{Fe}$ – $\text{Fe}'$  and  $\text{Fe}$ – $\text{Sb}$  distances and/or the  $\text{Fe}$ – $\text{Sb}$ – $\text{Fe}'$  bond angle (termed  $\delta$  in Fig. 1). As shown in Fig. 1, the  $\text{Fe}$ – $\text{Fe}'$  distance is larger for  $R = \text{Ba}$  while  $\delta$  is less, approaching  $90^\circ$ . Both tendencies would contribute to the suppression of the  $A$  feature intensity of the  $R = \text{Ba}$  system, as is observed. It must be appreciated, however, that the relative change of the structural parameters as a function of  $R$  is small and it is not clear whether such small changes could affect the  $\text{Fe}$   $3d$ – $\text{Sb}$   $5p$  orbital mixing in a significant manner. Based on EXAFS results, we turn now to a more detailed site-specific analysis of the structural parameters.

In Figs. 5(a)–5(f) we present the results of our EXAFS investigation at  $T = 10 \text{ K}$ . The application of EXAFS to the skutterudites contributed valuable information concerning bond disorder and the vibrational dynamics in this class of materials [35,39,40]. In Fig. 5(a) we present a broad view of the acquired spectra, comparing the detection from fluorescence and transmission. In the inset, we show the Fourier-transformed spectra in a broad range. In this paper, as presented in Figs. 5(b)–5(f), our analysis concentrates only on the region up to  $4 \text{ \AA}$  from the absorber, since we are interested only in evaluating details of the  $\text{Fe}$  coordination

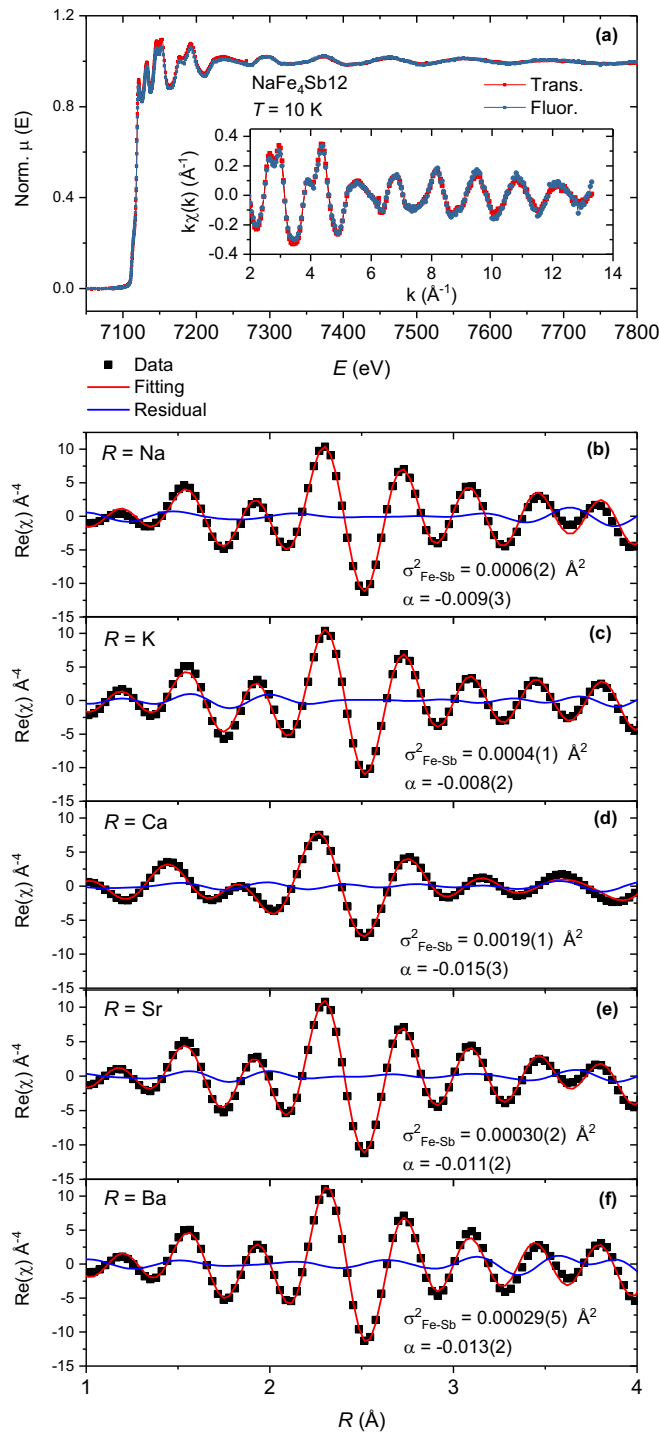


FIG. 5. (a) Representative Fe  $K$ -edge EXAFS spectra measured at  $T = 10$  K. In the inset, the Fourier transformed spectra in a broad interval are presented. (b)–(f) Fourier transformed spectra (squares) up to  $4 \text{ \AA}$  from the absorber and the theoretical model (solid red line) used to investigate the Fe coordination structure along the series ( $R = \text{Na, K, Ca, Sr, Ba}$ ).

structure. Single and multiple scattering paths relating Fe and Sb atoms and a single scattering Fe- $R$  path were taken into consideration to describe the data. The results for the obtained  $\sigma_{\text{Fe-Sb}}^2$ -correlated Debye-Waller factors and for the  $\alpha$  parameters adopted to describe the thermal contraction of the

Fe coordination are presented in the figures. All data could be well described without taking into account any particular distortion of the Fe coordination.

Electronic structure calculations suggest that the Fe-derived  $t_{2g}$  orbitals provide the main contribution to the system magnetic moments [26,27]. Therefore, Fe-Sb bond disorder is an important parameter in evaluating magnetic properties since it may affect the degeneracy of the  $t_{2g}$  orbitals and act as a local frustration mechanism of the  $t_{2g}$ -derived moments, quenching magnetic order. In principle, the analysis of the data at  $T = 10$  K reduces the effects of thermal motion and allows the analysis of the data to be inferred by comparing the  $\sigma_{\text{Fe-Sb}}^2$  for distinct fillers. However, the  $R\text{Fe}_4\text{Sb}_{12}$  skutterudites with light fillers present an unusual vibrational dynamics, as investigated in detail [37,41], which will affect the correlated Debye-Waller factors [35], rendering the comparison across the whole series inadequate.

A strong indication of this inadequacy is that the correlated Debye-Waller factors  $\sigma_{\text{Fe-R}}^2$  are larger for the  $R = \text{Na, K, and Ca}$  than for the  $R = \text{Sr and Ba}$  compounds, implying that the Fe- $R$  single scattering paths have little effect on the  $R = \text{Na, K, and Ca}$  spectra. In this sense, only the  $\sigma_{\text{Fe-Sb}}^2$  values for  $R = \text{Na, K, and Ca}$  are comparable, while the cases of the heavy fillers should be taken separately.

By inspecting the results for  $R = \text{Na, K, and Ca}$  one observes that  $\sigma_{\text{Fe-Sb}}^2$  is larger for  $R = \text{Ca}$  by one order of magnitude. This bond disorder may act as a local frustration parameter or, from the standpoint of the Stoner theory, it could simply reduce the Fe-Fe' exchange and thus the Stoner factor. In any case, this local parameter is likely more relevant to the suppression of the ferromagnetic order in  $\text{CaFe}_4\text{Sb}_{12}$  than the decrease of the density of states due the change of the filler cation, which is small when the cases  $\text{KFe}_4\text{Sb}_{12}$  and  $\text{CaFe}_4\text{Sb}_{12}$  are compared (Fig. 4).

Indeed, the large pre-edge intensity [see Fig. 4(b)] observed for  $\text{CaFe}_4\text{Sb}_{12}$  connects the local disorder to local electronic properties, since the large local disorder would favor the on-site Fe  $3d$ - $4p$  mixing, which is otherwise much too small due to symmetry constraints. This finding connects the unconventional vibrational dynamics of skutterudites to its electronic structure, which in some instances is known to affect their many-body electronic structure [42].

The absence of order in the cases of filling by Sr or Ba cannot be clarified in these terms. It could be rooted in the specifics of the Fe  $3d$ -Sb  $5p$  mixing and/or orbital occupation that, as suggested by the pre-edge analysis, is distinct for the  $R = \text{Na or K}$  and  $R = \text{Ca, Sr, or Ba}$  cases. In the context of the Fe  $3d$ -Sb  $5p$  hybridization, an intriguing possibility is offered by the interpretation [43,44] that the heavy quasiparticles at  $E_F$  develop out of a pseudogap, which is connected to the Kondo screening of the more localized Fe  $d$  states. The Kondo effect, being a many-body state, competes with the magnetic order.

The EXAFS analysis also indicates that the thermal contraction of the Fe coordination, as expressed by  $\alpha$ , is larger for the alkaline earth filled skutterudites. This is a point of relevance, since it implies a significant impact on the Fe coordination as a function of  $T$ . A more detailed EXAFS investigation will be the subject of future work. However, an interesting point related to our results deserves a final word: it is known

that the alkaline earth filled systems  $\text{CaFe}_4\text{Sb}_{12}$ ,  $\text{SrFe}_4\text{Sb}_{12}$ , and  $\text{BaFe}_4\text{Sb}_{12}$  are all strongly renormalized paramagnets, presenting robust ferromagnetic fluctuations. The bond shortening and increase in disorder observed in  $\text{CaFe}_4\text{Sb}_{12}$  is reminiscent of what was observed for  $\text{SmO}_{1-x}\text{F}_x\text{FeAs}$  [12], when quantum criticality is approached. Thus, the investigation of solid mixtures containing Na or K and Ca, Sr, or Ba is invited and may unveil some underlying quantum critical point controlling the physics of the  $R\text{Fe}_4\text{Sb}_{12}$  skutterudites.

#### IV. SUMMARY AND OUTLOOK

The electronic structure of the  $R\text{Fe}_4\text{Sb}_{12}$  ( $R = \text{Na}, \text{K}, \text{Ca}, \text{Sr}, \text{Ba}$ ) skutterudites were investigated by Fe  $K$ -edge XAS. With the support of FEFF calculations, we could interpret the specific contributions of the  $R$ , Fe, and Sb orbital states to the XAS spectra. The pre-edge was ascribed mainly to Fe  $3d$ -Sb  $5p$  orbital mixing, providing experimental evidence for strongly hybridized Fe-Sb states at  $E_F$ . This interpretation was further supported by the detailed analysis of the pre-edge intensity, which was shown to correlate with  $\gamma$  across the series, with the exception of the  $R = \text{Ca}$  case.

EXAFS analysis was carried out to investigate the coordination structure and no particular distortion of the Fe coordination was found. However, the Fe-Sb bond disorder for  $\text{CaFe}_4\text{Sb}_{12}$  was found to be significantly larger than for the  $R = \text{Na}$  or  $\text{K}$  cases, suggesting that the absence of a magnetically ordered state in  $\text{CaFe}_4\text{Sb}_{12}$  is due to Fe-Sb bond disorder.

In the analysis of the pre-edge transition, there is an indication that the pre-edge structure splits in two components for the paramagnetic systems, for which  $R = \text{Ca}, \text{Sr}, \text{or Ba}$ , but not for the ferromagnetically ordered skutterudites. In the cases of  $R = \text{Sr}$  or  $\text{Ba}$  the effect is particularly weak. However, comparison with FEFF simulations does support that the effect is likely intrinsic. The splitting suggests that the electronic states derived from Fe  $3d$ -Sb  $5p$  orbital mixing are more populated, or less localized, for the ferromagnetic systems.

In the context of the phenomenology of itinerant magnets hosting magnetic moments with weak local moment properties, our work reinforces the idea that the relevance of local properties, such as the electronic and coordination structures, may be a common thread to a large set of itinerant magnets.

#### ACKNOWLEDGMENTS

The authors acknowledge CNPEM-LNLS for the concession of beam time (Proposal No. 20160180). The XAFS2 beamline staff is acknowledged for assistance during the experiments. B.M. acknowledges financial support from CAPES (finance code 001) and the hospitality and financial support from the Department of Chemical Metal Sciences at the Max Planck Institute for Chemical Physics of Solids, Dresden, Germany. We thank A. Amon for his assistance with the sample XRD characterization.

- 
- [1] R. M. White, *Quantum Theory of Magnetism: Magnetic Properties of Materials* (Springer, Berlin, 2007).
- [2] J. Kübler, *Theory of Itinerant Electron Magnetism*, revised ed. (Oxford University Press, Oxford, 2009).
- [3] B. T. Matthias and R. M. Bozorth, *Phys. Rev.* **109**, 604 (1958).
- [4] B. T. Matthias, A. M. Clogston, H. J. Williams, E. Corenzwit, and R. C. Sherwood, *Phys. Rev. Lett.* **7**, 7 (1961).
- [5] E. Svanidze, J. K. Wang, T. Besara, L. Liu, Q. Huang, T. Siegrist, B. Frandsen, J. W. Lynn, A. H. Nevidomskyy, M. B. Gamza, M. C. Aronson, Y. J. Uemura, and E. Morosan, *Nat. Commun.* **6**, 7701 (2015).
- [6] Y. Kamihara, T. Watanabe, M. Hirano, and H. Hosono, *J. Am. Chem. Soc.* **130**, 3296 (2008).
- [7] E. M. Bittar, C. Adriano, T. M. Garitezi, P. F. S. Rosa, L. Mendonça-Ferreira, F. Garcia, G. d. M. Azevedo, P. G. Pagliuso, and E. Granado, *Phys. Rev. Lett.* **107**, 267402 (2011).
- [8] M. Merz, F. Eilers, T. Wolf, P. Nagel, H. van Loehneysen, and S. Schuppler, *Phys. Rev. B* **86**, 104503 (2012).
- [9] V. Balédent, F. Rullier-Albenque, D. Colson, J. M. Ablett, and J.-P. Rueff, *Phys. Rev. Lett.* **114**, 177001 (2015).
- [10] E. Granado, L. Mendonça-Ferreira, F. Garcia, G. d. M. Azevedo, G. Fabbri, E. M. Bittar, C. Adriano, T. M. Garitezi, P. F. S. Rosa, L. F. Bufaiçal, M. A. Avila, H. Terashita, and P. G. Pagliuso, *Phys. Rev. B* **83**, 184508 (2011).
- [11] J. Cheng, W. Chu, S. Liu, P. Dong, and Z. Wu, *J. Supercond. Novel Magn.* **27**, 9 (2014).
- [12] J. Cheng, P. Dong, W. Xu, S. Liu, W. Chu, X. Chen, and Z. Wu, *J. Synchrotron Radiat.* **22**, 1030 (2015).
- [13] M. Y. Hacisalihoglu, E. Paris, B. Joseph, L. Simonelli, T. J. Sato, T. Mizokawa, and N. L. Saini, *Phys. Chem. Chem. Phys.* **18**, 9029 (2016).
- [14] S. Lafuerza, H. Gretarsson, F. Hardy, T. Wolf, C. Meingast, G. Giovannetti, M. Capone, A. S. Sefat, Y.-J. Kim, P. Glatzel, and L. de' Medici, *Phys. Rev. B* **96**, 045133 (2017).
- [15] W. Jeitschko and D. Braun, *Acta Crystallogr., Sect. B: Struct. Crystallogr. Cryst. Chem.* **33**, 3401 (1977).
- [16] W. Schnelle, A. Leithe-Jasper, M. Schmidt, H. Rosner, H. Borrmann, U. Burkhardt, J. A. Mydosh, and Y. Grin, *Phys. Rev. B* **72**, 020402 (2005).
- [17] E. Matsuoka, K. Hayashi, A. Ikeda, K. Tanaka, T. Takabatake, and M. Matsumura, *J. Phys. Soc. Jpn.* **74**, 1382 (2005).
- [18] D. Berardan, E. Alleno, and C. Godart, *J. Magn. Magn. Mater.* **285**, 245 (2005).
- [19] J. Sichelschmidt, V. Voevodin, H. J. Im, S. Kimura, H. Rosner, A. Leithe-Jasper, W. Schnelle, U. Burkhardt, J. A. Mydosh, Y. Grin, and F. Steglich, *Phys. Rev. Lett.* **96**, 037406 (2006).
- [20] T. Takabatake, E. Matsuoka, S. Narazu, K. Hayashi, S. Morimoto, T. Sasakawa, K. Umeo, and M. Sera, *Physica B* **383**, 93 (2006).
- [21] H. Yamaoka, I. Jarrige, N. Tsujii, J.-F. Lin, T. Ikeno, Y. Isikawa, K. Nishimura, R. Higashinaka, H. Sato, N. Hiraoka, H. Ishii, and K.-D. Tsuei, *Phys. Rev. Lett.* **107**, 177203 (2011).

- [22] A. Leithe-Jasper, W. Schnelle, H. Rosner, N. Senthilkumaran, A. Rabis, M. Baenitz, A. Gippius, E. Morozova, J. A. Mydosh, and Y. Grin, *Phys. Rev. Lett.* **91**, 037208 (2003).
- [23] A. Leithe-Jasper, W. Schnelle, H. Rosner, M. Baenitz, A. Rabis, A. A. Gippius, E. N. Morozova, H. Borrmann, U. Burkhardt, R. Ramlau, U. Schwarz, J. A. Mydosh, Y. Grin, V. Ksenofontov, and S. Reiman, *Phys. Rev. B* **70**, 214418 (2004).
- [24] W. Schnelle, A. Leithe-Jasper, H. Rosner, R. Cardoso-Gil, R. Gumeniuk, D. Trots, J. A. Mydosh, and Y. Grin, *Phys. Rev. B* **77**, 094421 (2008).
- [25] R. Gumeniuk, H. Borrmann, A. Ormeci, H. Rosner, W. Schnelle, M. Nicklas, Y. Grin, and A. Leithe-Jasper, *Z. Kristallogr. - Cryst. Mater.* **225**, 531 (2010).
- [26] A. Leithe-Jasper, W. Schnelle, H. Rosner, W. Schweika, and O. Isnard, *Phys. Rev. B* **90**, 144416 (2014).
- [27] G. Xing, X. Fan, W. Zheng, Y. Ma, H. Shi, and D. J. Singh, *Sci. Rep.* **5**, 10782 (2015).
- [28] K. Momma and F. Izumi, *J. Appl. Crystallogr.* **41**, 653 (2008).
- [29] S. J. A. Figueroa, J. C. Mauricio, J. Murari, D. B. Beniz, J. R. Piton, H. H. Slepicka, M. F. d. Sousa, A. M. Espíndola, and A. P. S. Levinsky, *J. Phys.: Conf. Ser.* **712**, 012022 (2016).
- [30] J. J. Rehr and R. C. Albers, *Rev. Mod. Phys.* **72**, 621 (2000).
- [31] B. Ravel and M. Newville, *J. Synchrotron Radiat.* **12**, 537 (2005).
- [32] S. DeBeer George, P. Brant, and E. I. Solomon, *J. Am. Chem. Soc.* **127**, 667 (2005).
- [33] T. Yamamoto, *X-Ray Spectrom.* **37**, 572 (2008).
- [34] F. d. Groot, G. Vankó, and P. Glatzel, *J. Phys.: Condens. Matter* **21**, 104207 (2009).
- [35] F. Bridges, B. Car, L. Sutton, M. Hoffman-Stapleton, T. Keiber, R. E. Baumbach, M. B. Maple, Z. Henkie, and R. Wawryk, *Phys. Rev. B* **91**, 014109 (2015).
- [36] J. L. Feldman, D. J. Singh, and N. Bernstein, *Phys. Rev. B* **89**, 224304 (2014).
- [37] M. M. Koza, A. Leithe-Jasper, H. Rosner, W. Schnelle, H. Mutka, M. R. Johnson, M. Krisch, L. Capogna, and Y. Grin, *Phys. Rev. B* **84**, 014306 (2011).
- [38] M. Wilke, F. Farges, P.-E. Petit, G. E. Brown, and F. Martin, *Am. Mineral.* **86**, 714 (2001).
- [39] D. Cao, F. Bridges, P. Chesler, S. Bushart, E. D. Bauer, and M. B. Maple, *Phys. Rev. B* **70**, 094109 (2004).
- [40] F. Bridges, *Mod. Phys. Lett. B* **30**, 1630001 (2016).
- [41] M. M. Koza, M. R. Johnson, R. Viennois, H. Mutka, L. Girard, and D. Ravot, *Nat. Mater.* **7**, 805 (2008).
- [42] P. A. Venegas, F. A. Garcia, D. J. Garcia, G. G. Cabrera, M. A. Avila, and C. Rettori, *Phys. Rev. B* **94**, 235143 (2016).
- [43] S.-i. Kimura, T. Mizuno, H. Im, K. Hayashi, E. Matsuoka, and T. Takabatake, *Phys. Rev. B* **73**, 214416 (2006).
- [44] S.-i. Kimura, H. Im, T. Mizuno, S. Narazu, E. Matsuoka, and T. Takabatake, *Phys. Rev. B* **75**, 245106 (2007).